SUPPLEMENTARY INFORMATION

1D Mn(III) Coordination Polymers Exhibiting Chiral Symmetry Breaking and Weak Ferromagnetism

Aoi Hara,[a] Sotaro Kusumoto,[a] Yoshihiro Sekine,[a,b] Jack Harrowfield,[c] Yang Kim,[a] Shinya Hayami,[a,d] Masaaki Nakamura*[a]*

[a]Department of Chemistry, Graduate School of Science and Technology, Kumamoto University, 2-39-1 Kurokami, Chuo-ku, Kumamoto 860-8555, Japan.

[b]Priority Organization for Innovation and Excellence, Kumamoto University, 2-39-1 Kurokami, Chuo-ku, Kumamoto 860-8555, Japan.

[c]ISIS, Université de Strasbourg, 8 allée Gaspard Monge, 67083 Strasbourg, France.

[d]Institute of Industrial Nanomaterials (IINa), Kumamoto University, 2-39-1 Kurokami, Chuo-ku, Kumamoto 860-8555, Japan.

Corresponding author: S. Hayami
E-mail: hayami@kumamoto-u.ac.jp

Syntheses

All reagents and solvents were purchased from Tokyo Kasei Co. and Wako Pure Chemical Industries and used without further purification. Elemental analyses (C,H,N) were carried out on a J-SCIENCE LAB JM10 analyzer at the Instrumental Analysis Centre in Kumamoto University. 2-Aminobenzaldehyde for ligands synthesis and complex **1** were prepared according to previously reported method. [SI1]

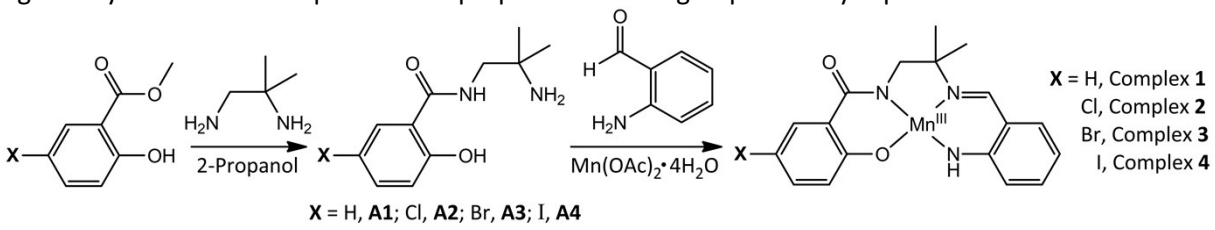

Scheme 1. Preparation of Mn complexes.

***N*-(2-amino-2-methylpropyl)-5-chloro-2-hydroxybenzamide (A2)**
Methyl 5-chlorosalicylate (1.87 g, 10 mmol) in 2-propanol (80 mL) was added dropwise with stirring over 1 h to 2-methyl-1,2-propanediamine (0.88 g, 10 mmol) in propanol (15 mL). The mixture was stirred for 2 days at ambient temperature. The resulting white precipitate was collected by filtration, washed with a small amount of 2-propanol, and dried under reduced pressure. Yield: 2.08 g (85.7 %). ^{1}H NMR (500 MHz, DMSO-d_6): δ 0.53 (s, 6H, C*H*3), 3.26 (s, 2H, C*H*2), 6.02 (d, 1H, C(3)*H*), 6.53 (d, 1H, C(4)*H*), 7.17 (s, 1H, C(6)*H*), 11.00 (s, 1H, O*H*). Characteristic IR: 3280, 3126, 3120, 2967, 1635, 1580, 1559 cm^{-1}.

***N*-(2-amino-2-methylpropyl)-5-bromo-2-hydroxybenzamide (A3)**
A3 was prepared in the same method as above using methyl 5-bromosalicylate (2.31 g, 10 mmol) and 2-methyl-1,2-propanediamine (0.88 g, 10 mmol). Yield: 2.08 g (72%). ^{1}H NMR (500 MHz, DMSO-d_6): δ 1.16 (s, 6H, C*H*3), 3.35 (s, 2H, C*H*2), 6.48 (d, 1H, C(3)*H*), 7.11 (d-d, 1H, C(4)*H*), 7.78 (d, 1H, C(6)*H*). Characteristic IR absorptions: 3246, 2968, 1635, 1589, 1548 cm^{-1}.

***N*-(2-amino-2-methylpropyl)-5-iodo-2-hydroxybenzamide (A4)**
A4 was prepared in the same method as above using methyl 5-iodosalicylate (2.78 g, 10 mmol) and 2-methyl-1,2-propanediamine (0.88 g, 10 mmol). Yield: 2.04 g (61%). ^{1}H NMR (500 MHz, DMSO-d_6): δ 0.98 (s, 6H, C*H*3), 3.16 (s, 2H, C*H*2), 6.16 (d, 1H, C(3)*H*), 7.02 (d-d, 1H, C(4)*H*), 7.72 (d, 1H, C(6)*H*). Characteristic IR absorptions: 3321, 2963, 1612, 1595, 1556 cm^{-1}.

[Mn(L^{Cl})] (2).
A mixture of **A2** (0.24 g, 1.0 mmol) and 2-aminobenzaldehyde (0.12 g, 1.0 mmol) in ethanol (40 mL) was stirred for 1 h at 70 °C. $Mn(OAc)_2{\cdot}4H_2O$ (0.25 g, 1.0 mmol) in ethanol (10 mL) was added to the resulting solution and stirred for 2 h at 70 °C, then cooled to ambient temperature. The brown powder was filtered and recrystallized to give brown plate crystals suitable for a structure determination. Yield: 0.118 g (30%). Anal. calc. for [Mn**L^{Cl}**]·0.5H_2O ($C_{18}H_{17}MnClN_3O_2{\cdot}0.5H_2O$): C, 53.15; H, 4.46; N, 10.33%. Found: C, 53.40; H, 4.78; N, 10.24%. Characteristic IR: 3342, 2964, 1612, 1596, 1566, 1531 cm^{-1}.

[Mn(L^{Br})] (3).
Complex **3** was prepared in the same method as above using **A3** (0.29 g, 0.1 mmol). Brown plate crystals suitable for a structure determination were obtained by recrystallization in methanol. Yield: 0.108 g (24%). Anal. calc. for [Mn**L^{Br}**] ($C_{18}H_{17}MnBrN_3O_2$): C, 48.89; H, 3.88; N, 9.50. Found: C, 48.66; H, 4.05; N, 9.20%. Characteristic IR absorptions: 3342, 1612, 1593, 1570, 1541 cm^{-1}.

[Mn(L^{I})] (4).

Complex **4** was prepared in the same method as above using **A4** (0.33 g, 1.0 mmol). Brown plate crystals suitable for a structure determination were obtained by recrystallization in methanol. Yield: 0.190 g (39%). Anal. calc. for [Mn**L**^{I}] ($C_{18}H_{17}MnIN_3O_2$): C, 44.19; H, 3.50; N, 8.59. Found: C, 44.05; H, 3.57; N, 8.49%. Characteristic IR absorptions: 3327, 1610, 1587, 1558, 1525 cm^{-1}.

Physical measurements

Single-crystal X-ray diffraction data for both enantiomers of **2**-**4** were collected with a Rigaku XtaLAB mini II diffractometer. The structures were solved by direct methods (SHELXT[SI2]) and refined by full-matrix least-squares refinement using the SHELXL[SI3] program. Hydrogen atoms were refined geometrically using a riding model. Crystallographic data for **2**-**4** (both enantiomers) are summarised in Table S1. Powder X-ray diffraction data (PXRD) were collected on a RIGAKU MiniFlex II ultra (30 kV/15 mA) X-ray diffractometer using Cu Kα radiation (λ = 1.5406 Å) in the 2θ range of 2°−30° with a step width of 1.0°. Variable-temperature dc magnetic susceptibility, ac magnetic susceptibility measurements, and field dependence of magnetization were performed on a superconducting quantum interference device (SQUID) magnetometer (Quantum Design MPMS XL). Circular dichroism (CD) spectra of KBr pellets containing the samples were measured by a JASCO J-720 spectrophotomer at R.T.

Supplementary data

Table S1. Crystallographic data for both enantiomers of **2–4**.

Compound	**2(*M*)**	**2(*P*)**	**3(*M*)**	**3(*P*)**	**4(*M*)**	**4(*P*)**
formula	$C_{18}H_{17}ClMnN_3O_2$	$C_{18}H_{17}ClMnN_3O_2$	$C_{18}H_{17}BrMnN_3O_2$	$C_{18}H_{17}BrMnN_3O_2$	$C_{18}H_{17}IMnN_3O_2$	$C_{18}H_{17}IMnN_3O_2$
formula weight	397.75	397.75	442.20	442.20	489.20	489.20
crystal system	Orthorhombic	Orthorhombic	Orthorhombic	Orthorhombic	Orthorhombic	Orthorhombic
space group	$P2_12_12_1$	$P2_12_12_1$	$P2_12_12_1$	$P2_12_12_1$	$P2_12_12_1$	$P2_12_12_1$
a / Å	7.8674(11)	7.8303(3)	7.8656(7)	7.9237(4)	9.5006(4)	9.5303(3)
b / Å	12.6283(19)	12.6301(6)	12.7295(6)	12.7678(5)	10.4519(4)	10.3905(3)
c / Å	16.991(3)	17.0111(9)	17.3852(10)	17.3798(10)	17.3947(6)	17.3403(5)
α / º	90.0000	90.0000	90.0000	90.0000	90.0000	90.0000
β / º	90.0000	90.0000	90.0000	90.0000	90.0000	90.0000
γ / º	90.0000	90.0000	90.0000	90.0000	90.0000	90.0000
V / Å^3	1688.1(4)	1682.35(14)	1740.7(2)	1758.28(15)	1727.28(11)	1717.12(9)
Z	4	4	4	4	4	4
T / K	223	120	120	223	223	120
R_1 [I > 2σ(I)]	0.0701	0.0456	0.0392	0.0418	0.0191	0.0220
wR_2 [I > 2σ(I)]	0.1157	0.0876	0.0747	0.0661	0.0490	0.0416
R_1 (all data)	0.1414	0.0627	0.0462	0.0558	0.0201	0.0247
wR_2 (all data)	0.1391	0.0937	0.0767	0.0691	0.0494	0.0424
G.O.F.	0.9422	1.0078	1.0455	1.0272	1.0394	1.0370
Flack χ parameter	0.00(5)	-0.02(3)	0.026(12)	0.031(13)	-0.011(17)	-0.02(2)
CCDC	2060011	2060012	2060013	2060014	2060015	2060016

Table S2. Characteristic bond distances data for both enantiomers of **2–4**.

	2 (*M*)	**2 (*P*)**	**3 (*M*)**	**3 (*P*)**	**4 (*M*)**	**4 (*P*)**
Mn -O_{phenol}	1.861(4)	1.866(3)	1.872(2)	1.869(2)	1.8695(19)	1.874(2)
Mn -$N_{(amide)}$	1.947(5)	1.947(3)	1.954(3)	1.945(3)	1.952(2)	1.955(3)
Mn – $N_{(imine)}$	1.994(5)	1.991(3)	1.989(3)	1.988(3)	1.991(2)	1.998(2)
Mn –$N_{(amine)}$	1.913(6)	1.921(3)	1.915(3)	1.914(3)	1.918(2)	1.924(3)

Mn –$O_{(amide)}$	2.103(4)	2.102(3)	2.0813(	2.083(3)	2.113(2)	2.117(2)
O=$C_{(amide)}$	1.273(7)	1.275(4)	1.265(4)	1.260(4)	1.275(3)	1.280(4)
Mn…$Mn_{shortest}$	6.075	6.078	6.001	6.004	5.772	5.765

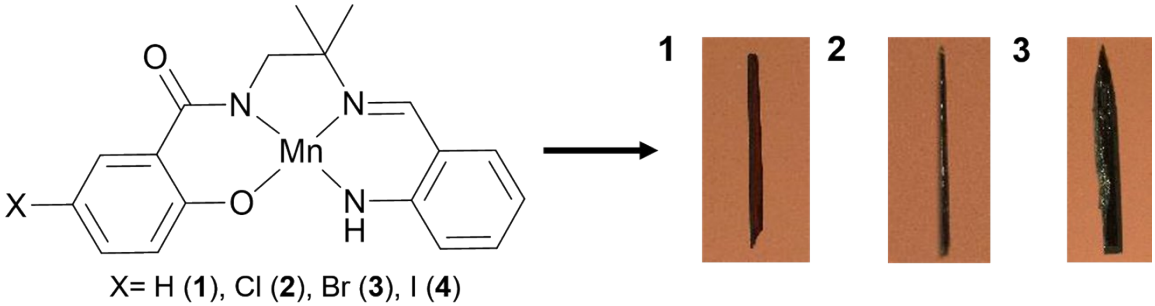

X= H (**1**), Cl (**2**), Br (**3**), I (**4**)

Fig. S1 Thin plate-like crystals of **1-3** obtained by slow evaporation in methanol.

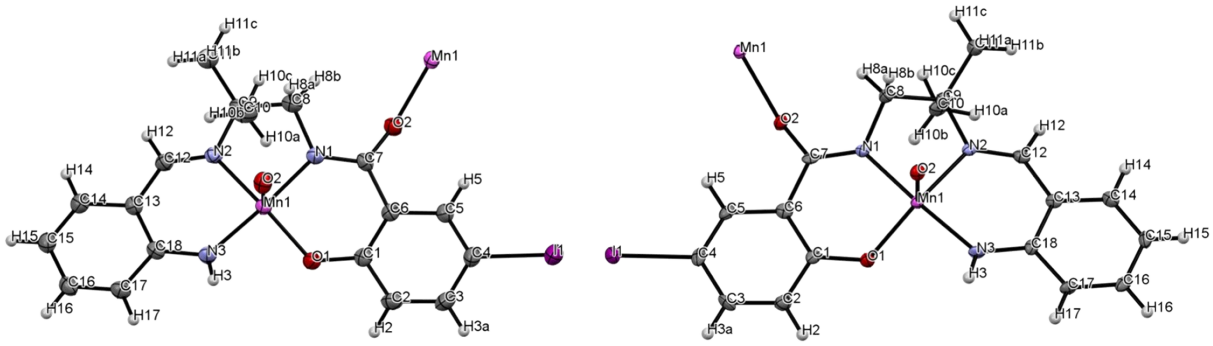

Fig. S2 The molecular structures of **4**, showing displacement ellipsoids at the 50% probability level.

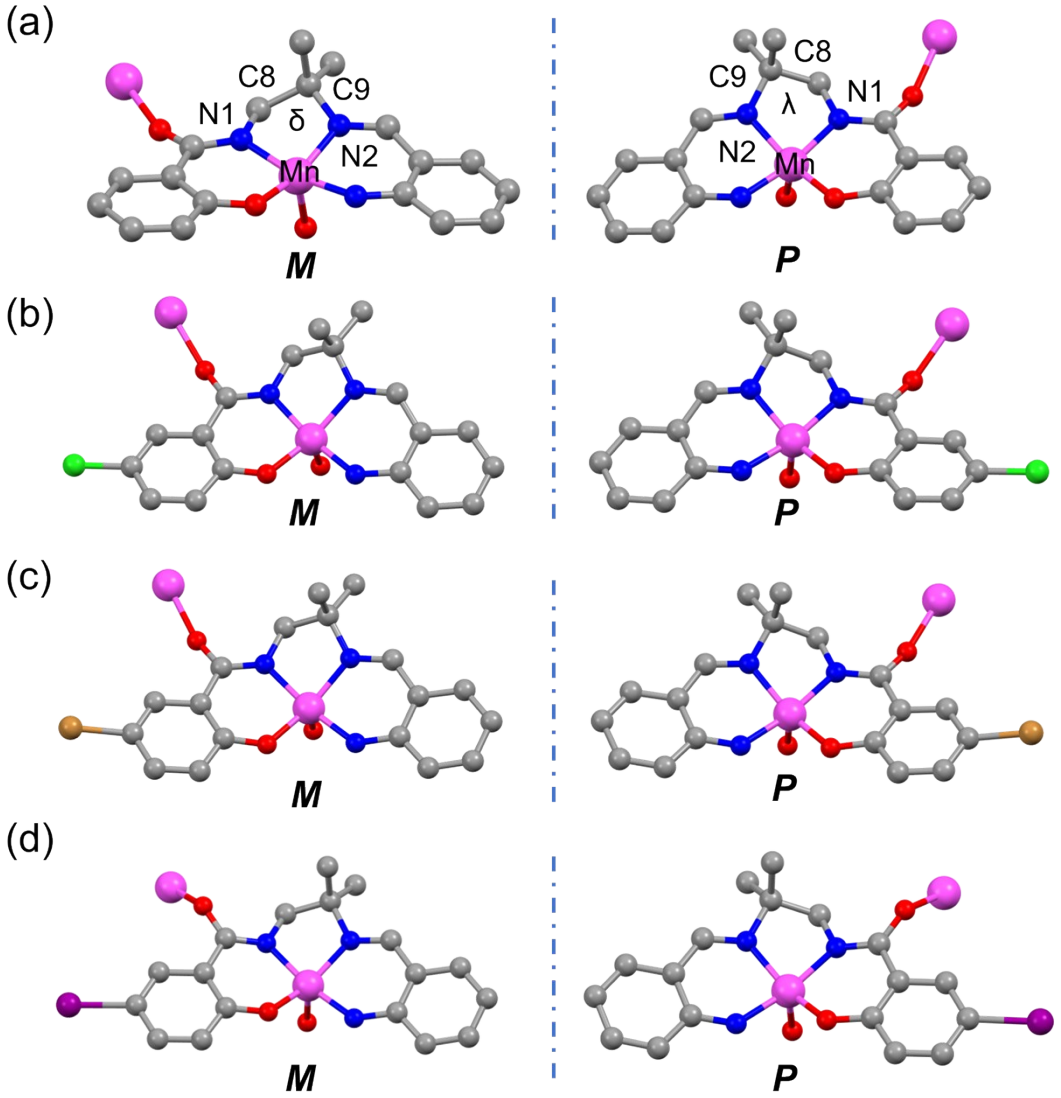

Fig. S3 Structures of both enantiomers of **1**(a), **2**(b), **3**(c) and **4**(d).

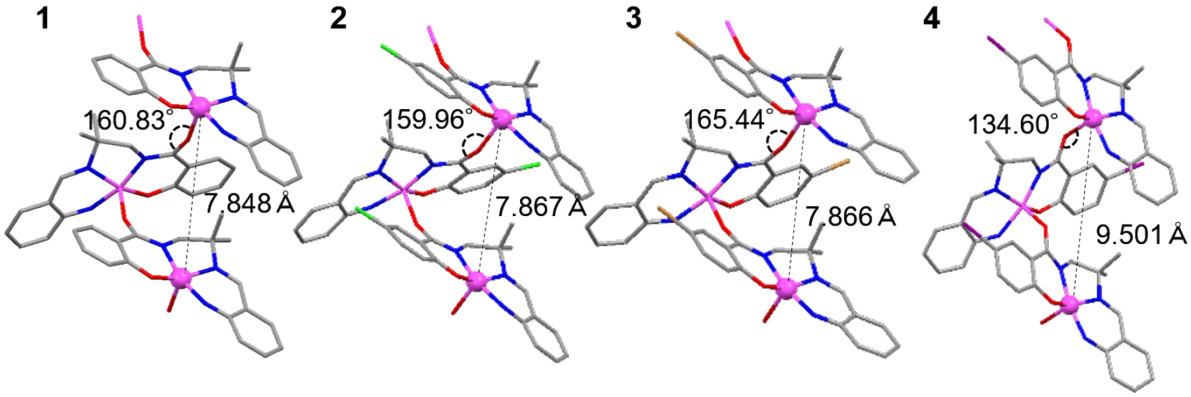

Fig. S4 Distances of helix pitches and ∠Mn-O-C of **1**–**4**.

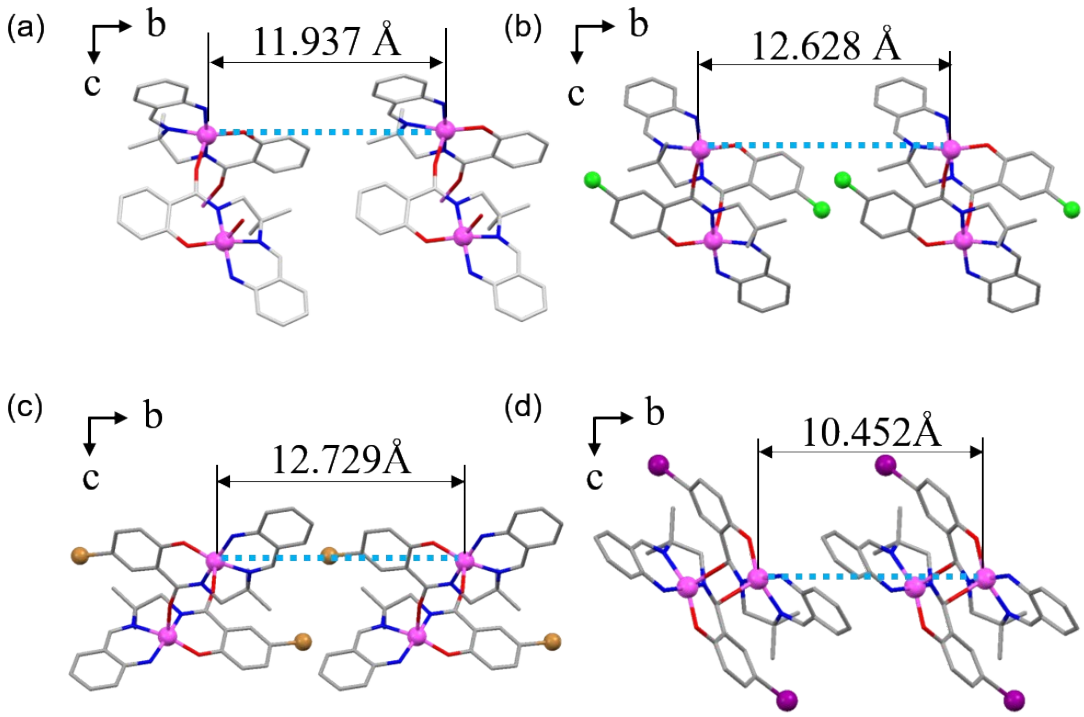

Fig. S5 The shortest distances between two interchain Mn(III) ions for **1**(a), **2**(b), **3**(c) and **4**(d).

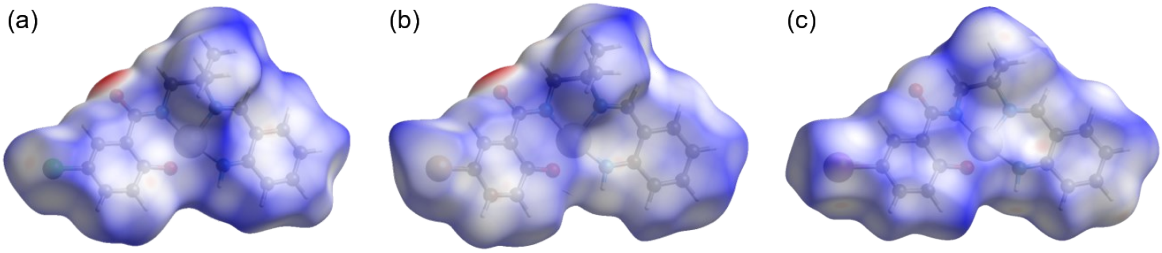

Fig. S6 Hirshfeld surfaces for complex **2**(a), **3**(b) and **4**(c).

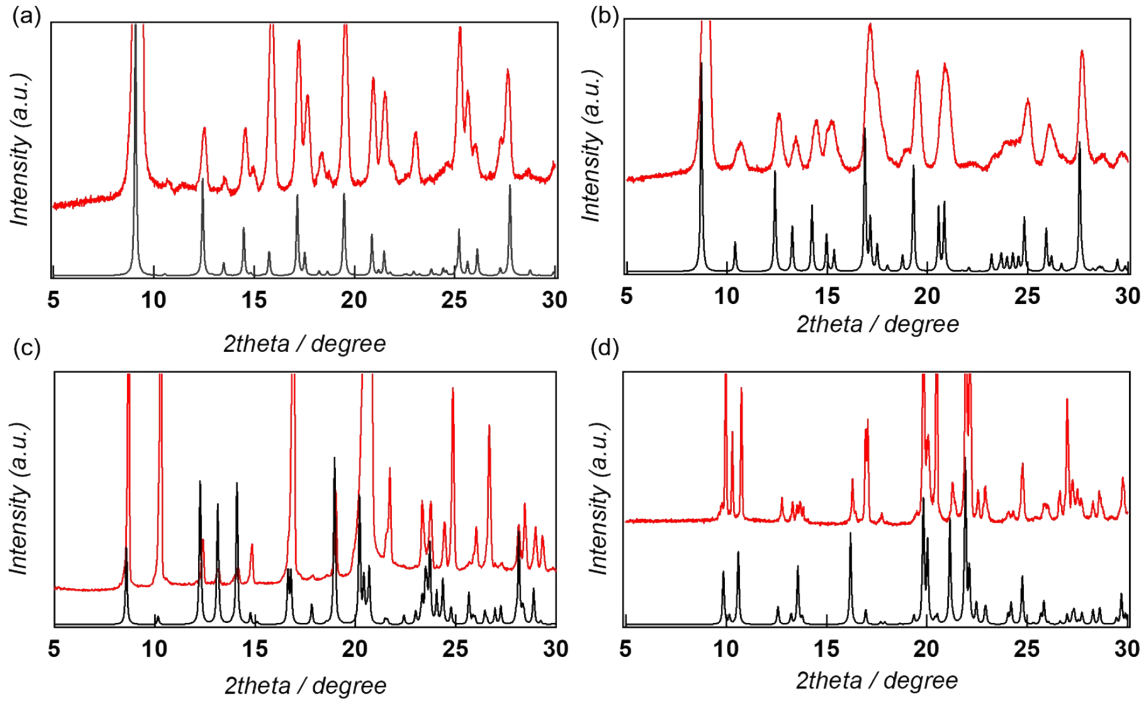

Fig. S7 Experimental (red) and simulated (black) PXRD patterns measured for microcrystalline samples of **1**(a), **2**(b), **3**(c) and **4**(d).

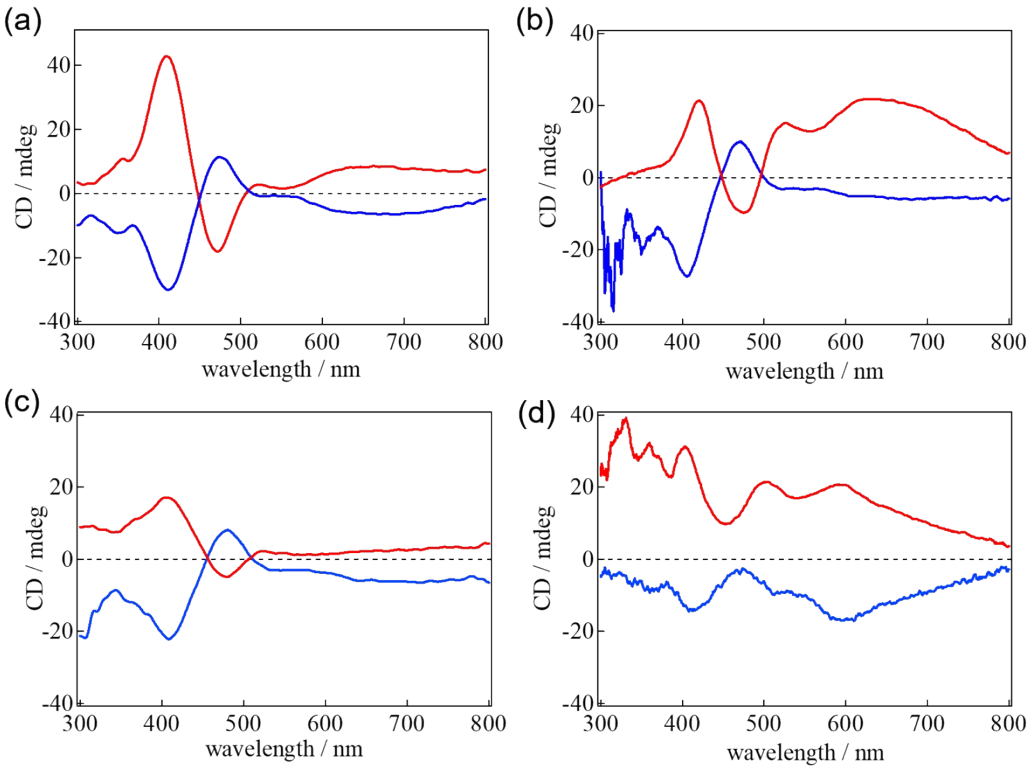

Fig. S8 Solid-state CD spectra for enantiomerically pure crystals of **1**(a), **2**(b), **3**(c) and **4**(d) (***P*** isomer in red line and ***M*** in blue) after X-ray crystallographic characterization.

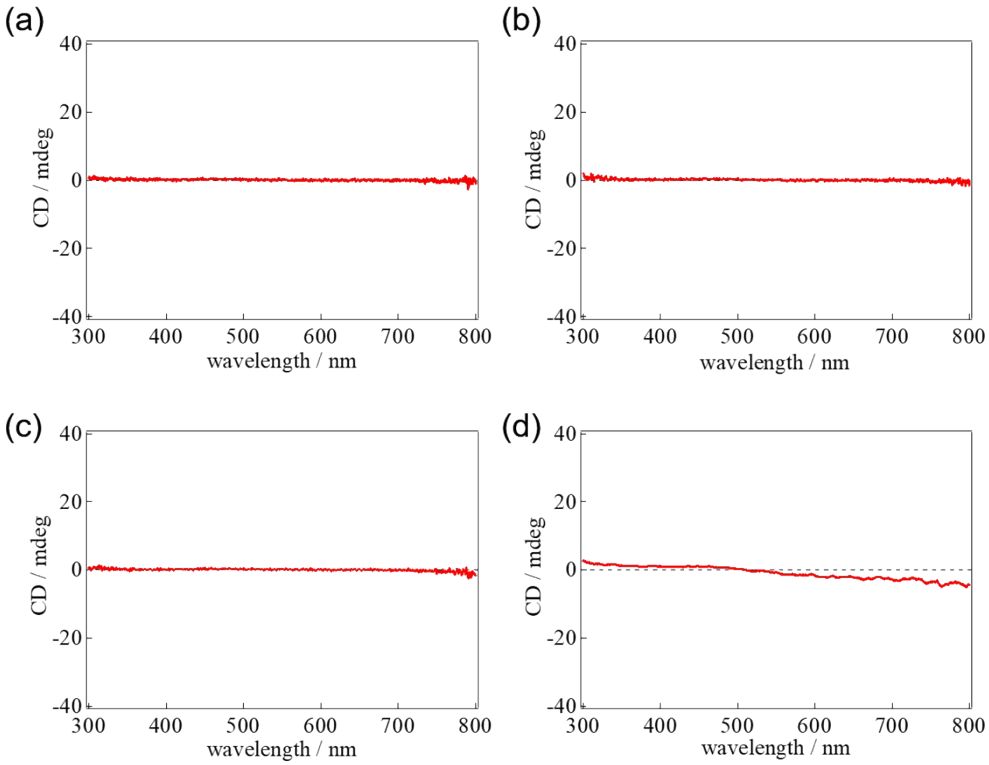

Fig. S9 Solution CD spectra for coordination polymers of **1**(a), **2**(b), **3**(c) and **4**(d) in methanol.

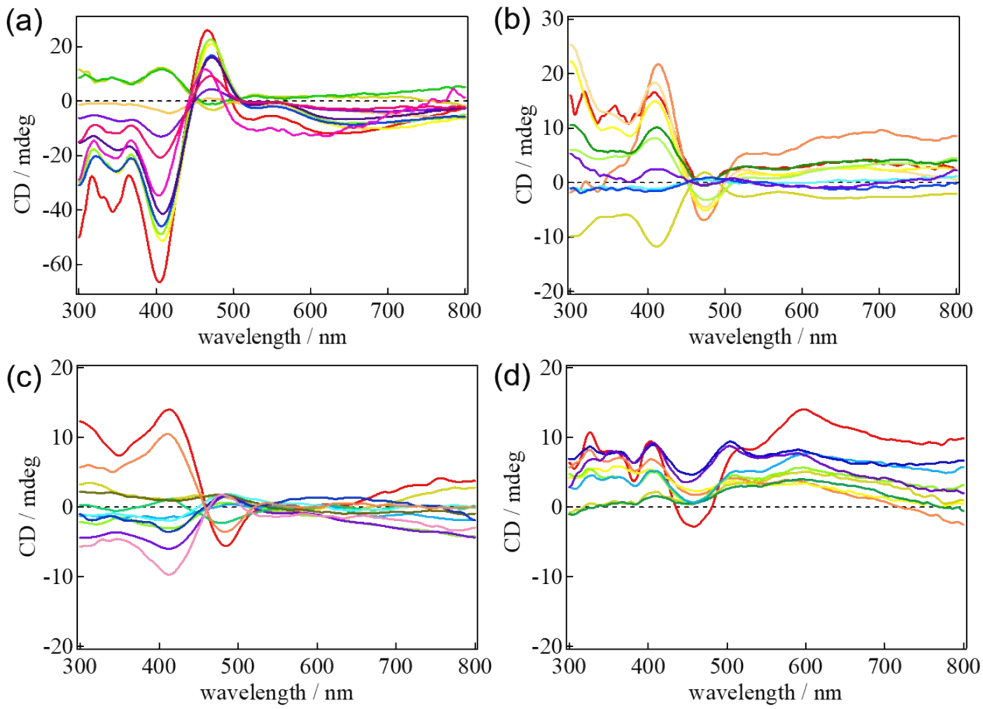

Fig. S10 Solid-state CD spectra for at least 10 KBr disks. Each of them was measured from all bulk crystalline products obtained under recrystallisation experiment of **1**(a), **2**(b), **3**(c) and **4**(d) without external stimuli.

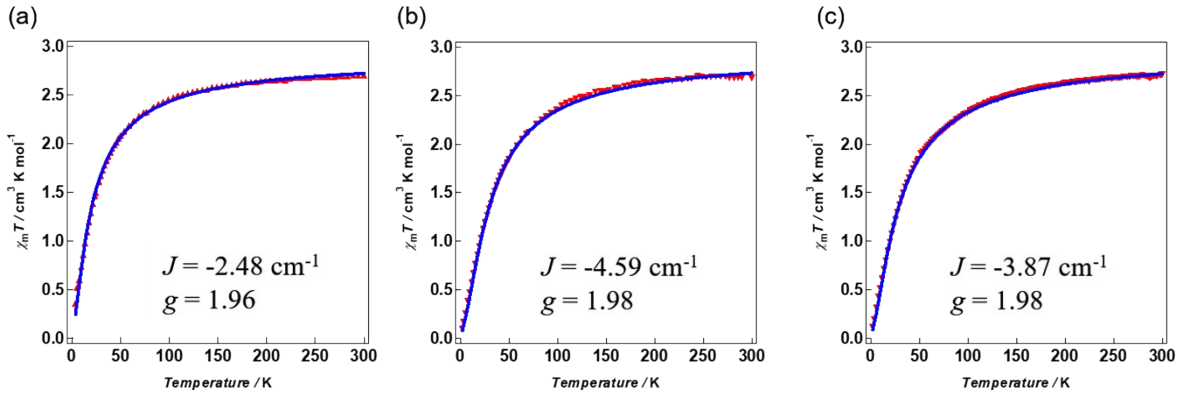

Fig. S11 The magnetic susceptibility of complexes **1**(a) , **2**(b), and **3**(c) has been measured at 2-300 K under 5.0 KOe applied magnetic field. The experimental data from 300 to 2 K were fitted based on a linear chain assuming Heisenberg isotropic coupling according to Fisher's expression for S = 2 (eqn. (1) and (2)). The solid blue line represents the best fit and the fitting results are shown inside each graph.

$$\chi = \left[\frac{Ng^2\mu^2 S(S+1)}{3k}\right]\left[\frac{1+u}{1-u}\right] \qquad (1)$$

$$u = \coth\left[\frac{JS(S+1)}{kT}\right] - \left[\frac{kT}{JS(S+1)}\right](S=2)$$

$$\chi_{MFA} = \frac{\chi}{1-\chi(zJ'/Ng^2\mu^2)} \qquad (2)$$

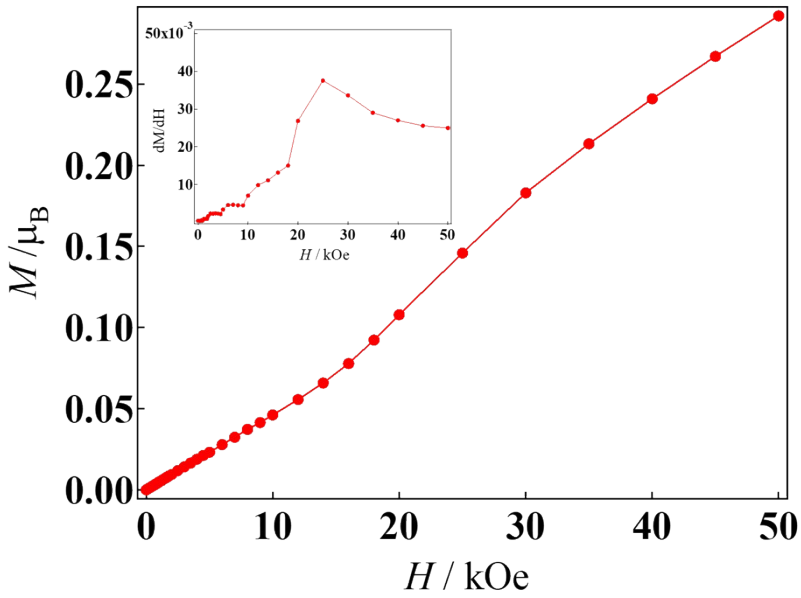

Fig. S12 Magnetization from 0 to 50 kOe at 2 K. The dM/dH plot is shown as an inset.

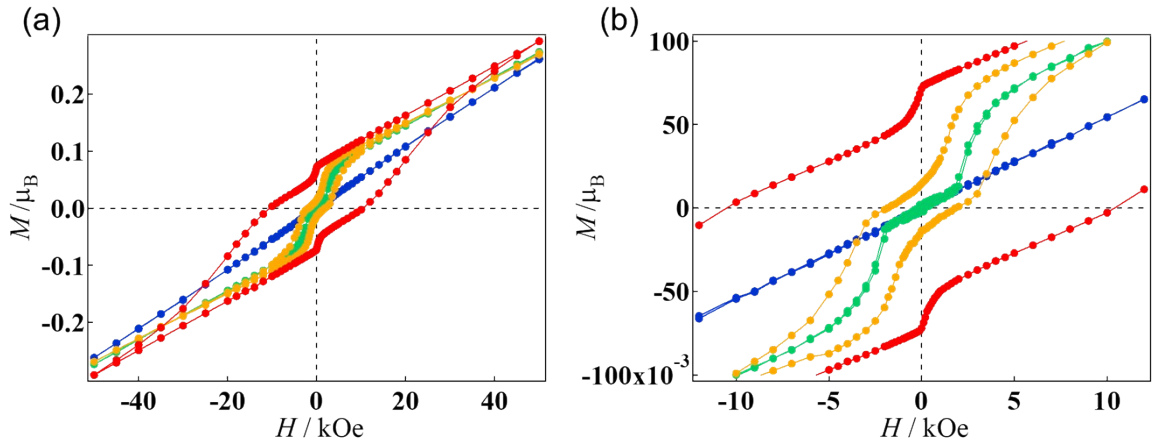

Fig. S13 *M* vs. *H* plots for **4** at 16K (blue), 10K (green), 6K (yellow) and 2K (red).

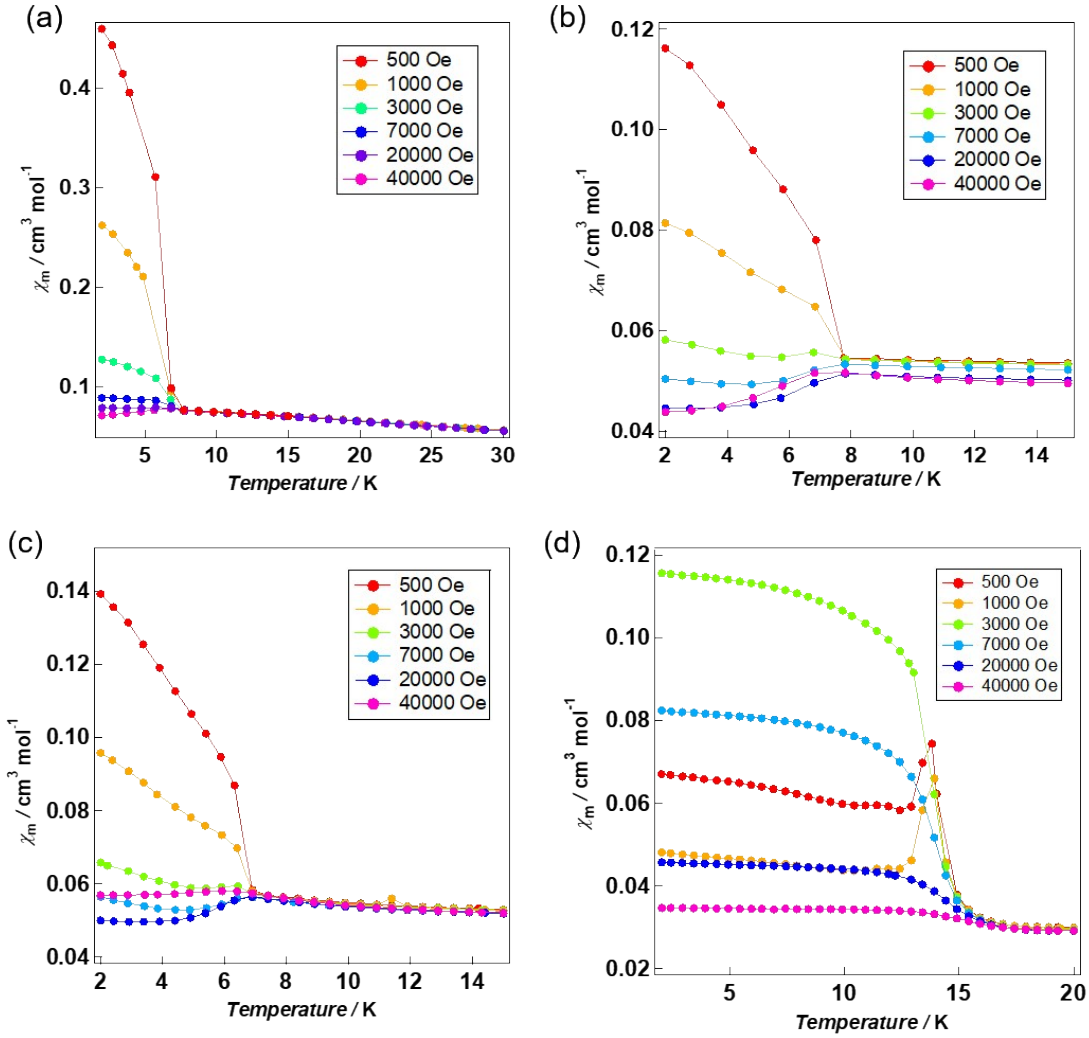

Fig. S14 The χ_m vs. *T* plots in a field range of 0.5–40 kOe for **1**(a)–**4**(d).

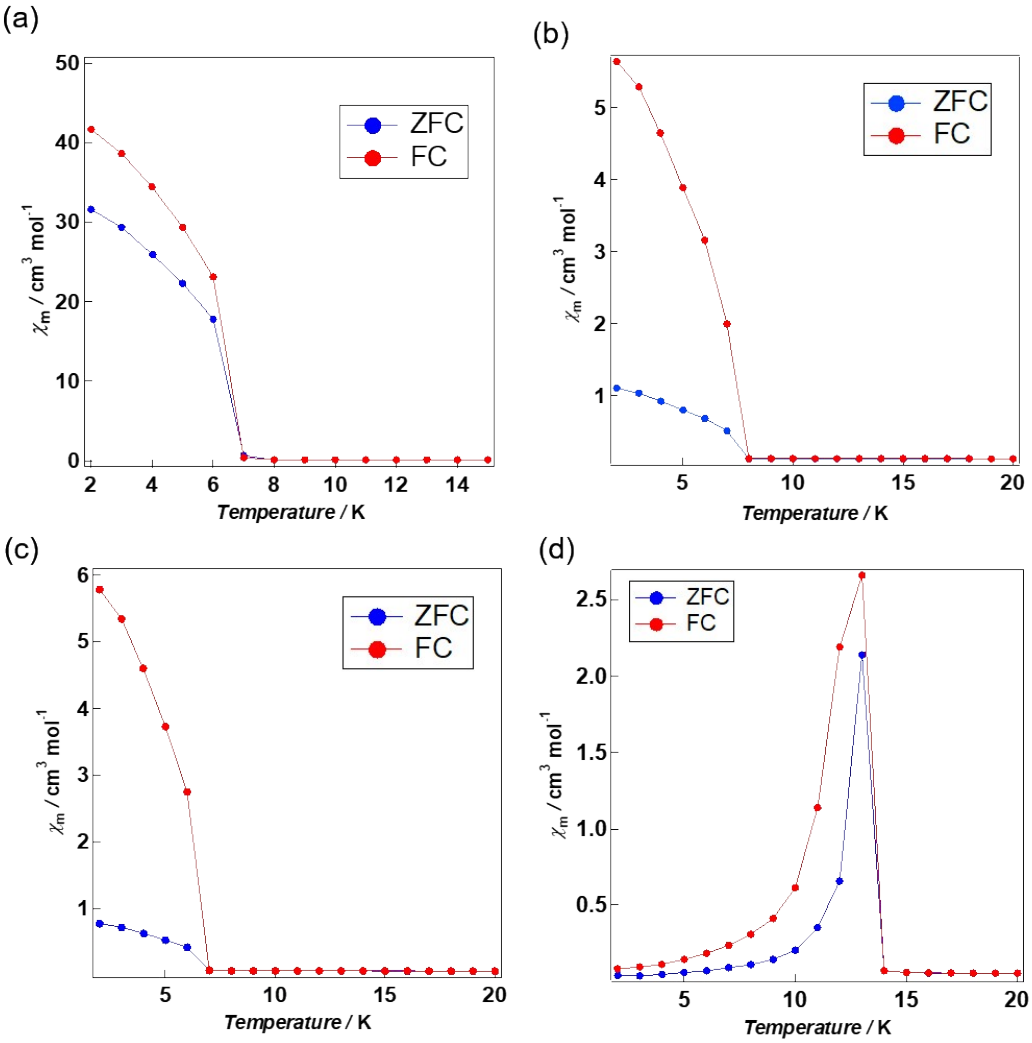

Fig. S15 Zero-field-cooled magnetization (ZFC) and field-cooled magnetization (FC) curves under an applied field of 5 Oe for **1**(a)–**4**(d).

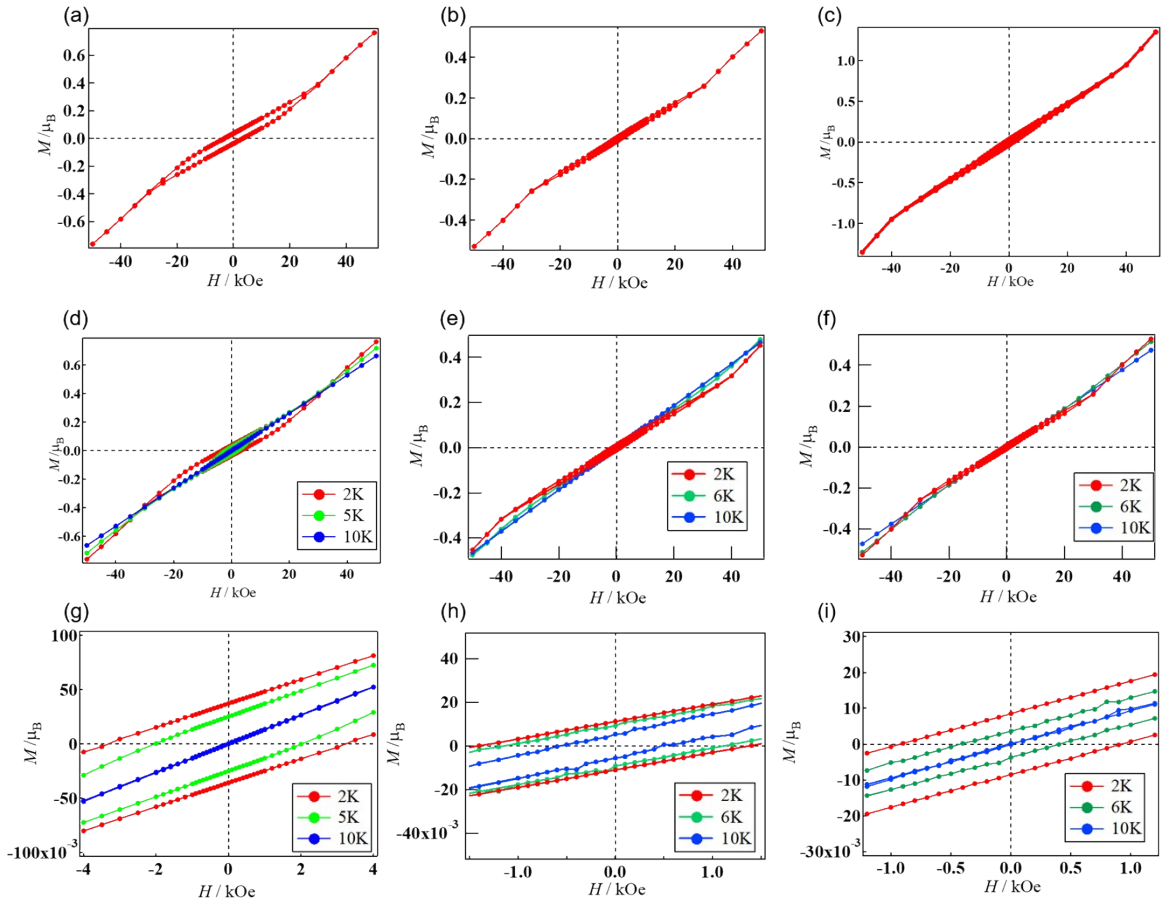

Fig. S16 The field dependence of the magnetization of **1**(a), **2**(b) and **3**(c) at 2K in the range −50 kOe to 50 kOe. The field dependence of the magnetization at variable temperature and the enlarged figures of the hysteresis loops of **1**(d, g), **2**(e, h) and **3**(f, i) in the range −50 kOe to 50 kOe.

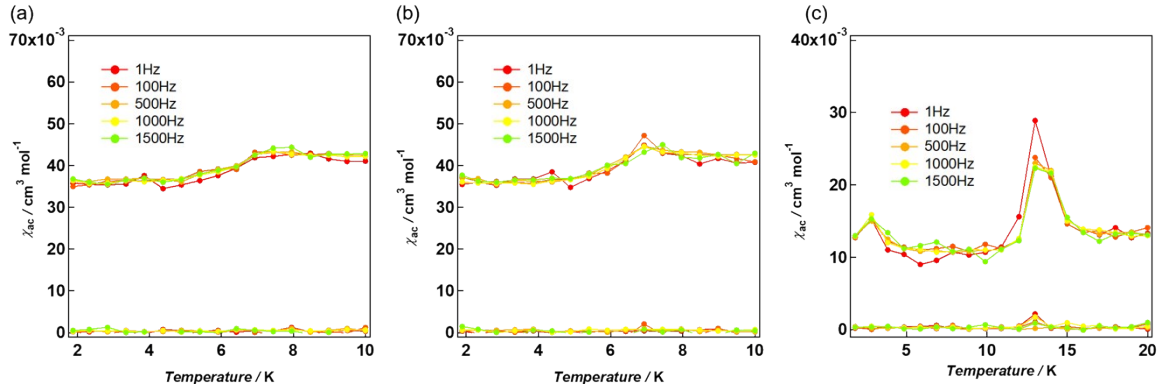

Fig. S17 Temperature dependence of ac susceptibilities of **2**(a), **3**(b) and **4**(c) in-phase (χ_m') and out-of-phase (χ_m'') at different frequencies under zero dc field.

References

[1] a) S. Kusumoto, A. Koga, F. Kobayashi, R. Ohtani, Y. Kim, L. F. Lindoy, S. Hayami, M. Nakamura, *Dalton Trans*., 2019, **48**, 8617-8622; b) L. T. Taylor, S. C. Vergez, D. H. Busch, *J. Am. Chem. Soc.*, 1966, **88**, 3170–3171.

[2] G. M. Sheldrick, SHELXT – Integrated Space-Group and Crystal-Structure Determination, Acta Crystallogr., Sect. A: Found. Adv., **2015**, *71*, 3–8.

[3] G. M. Sheldrick, Crystal Structure Refinement with SHELXL. Acta Crystallogr Sect. C **2015**, *71*, 3–8.